Saddle dolomite: a new view of its nature and origin

ALISON SEARL

School of Earth Sciences, University of Birmingham, P.O. Box 363, Birmingham, B15 2TT

Abstract

Saddle dolomite is a common product of late-stage diagenesis and hydrothermal activity. It has been suggested that during growth Ca enrichment occurs towards crystal edges leading to a lattice expansion relative to face centres. However, backscatter scanning electron microscopy of eight samples has revealed that, instead of edge associated Ca enrichment, saddle dolomites have a series of edge associated Mg enriched wedges, between 5 and 20 μm thick and 300 μm long. Wedge geometry implies development of extra lattice layers at edges relative to face centres. It is suggested that the wedges develop during rapid, transport-controlled, crystal growth. The wedges possibly reflect a switching from continuous growth across the face to edge-nucleated growth as the boundary layer solution becomes progressively depleted. Continuous growth might be reinstigated through convective turnover of the boundary layer presenting fresh solution to the growing crystal.

KEYWORDS: saddle dolomite, oscillatory zoning, crystal growth mechanisms, BSEM imaging.

Introduction

SADDLE dolomite is characterized by curved crystal faces and sweeping extinction (Fig. 1) indicative of a warped crystal lattice (Radke and Mathis, 1980). It is a common product of late-stage diagenesis and hydrothermal activity and normally occurs as pore-filling cement or in veins. It has also been reported as a replacement product in some dolomitized limestones (e.g. Hird *et al.*, 1987). Despite its relatively common occurrence, the origin of saddle dolomite is poorly understood. Radkhe and Mathis (1980) suggest that it forms at temperatures between 60 and 150 °C and that the saddle form reflects preferential Ca uptake towards crystal corners, which causes lattice expansion relative to face centres. More recent TEM work has revealed the presence of thin (<100 nm) calcitic laths within the saddle dolomite lattice which are believed to contribute to the overall crystallographic distortion (Barber *et al.*, 1985). The calcitic laths are subparallel to {10T4} faces of rhombic dolomite) and have branching dendritic morphologies which Barber *et al.* (1985) suggest indicates precipitation from a Ca-rich solution.

In this study eight saddle dolomite samples were examined using backscatter scanning electron microscopy (BSEM). This revealed a previously undescribed pattern of compositional variation in which a series of relatively Mg enriched wedges is developed in association with propagating crystal edges. These are of obvious significance in understanding the growth mechanisms leading to saddle dolomite and, therefore, ultimately in determining the geochemical environments of saddle dolomite precipitation.

Samples

The saddle dolomite samples came from five localities in the Lower Carboniferous, three in Fife, Scotland, and two in south Wales, and from the Permian at one locality in northern England (Table 1). All the samples were void filling and three were associated with sulphide mineralization.

Methods

The BSEM imaging and analyses were carried out on a Jeol superprobe 733, operating at 15 kV with a beam current of 1.5×10^{-2} μmA. Non-carbonate standards were used which restricts the absolute comparison of dolomite compositions reported here with those of other workers. However, the analyses are sufficient to enable interpretation of the BSEM images. Analytical precision is difficult to assess because of the problem of volatilization: Fe-rich samples appeared to be

Mineralogical Magazine, December 1989, Vol. 53, pp. 547–555

Table 1: samples

Sample number			National Grid Reference
WL7	St Monans White Limestone	Lower Limestone Group, Lower Carboniferous Fife	NO 538022
FF1)	Charlestown Main Limestone		NO 536019
FF2)			NO 536019
KH 42	Upper Kinniny Limestone		NT 280889
AS1	Base of Oolite Group	Lower Carboniferous South Wales	ST 082142
G113135	Gully Oolite		SS 534879
AS4)	Marl Slate, Permian:	NCB Core Yorkshire	SE 6721714791
AS5			

most susceptible to volatization and have recalculated totals (i.e. minus CO_2) of only about 97 wt. ‰. Defocussing the beam only further lowers totals.

Results

The total range of dolomite compositions (Fig. 2) are from 49 to 56.3 mol.% $CaCO_3$ and from 0 to 21.2 mol.% $FeCO_3$. In individual samples compositional ranges show a variation of up to 3 mol.% $CaCO_3$ and up to 5 mol. % $FeCO_3$.

Viewed in backscattered electron emission crystals have a consistent characteristic zonation in which series of paired wedges of lower average atomic number are present in the crystal (Fig. 3). In individual samples both wedges and host tend to have fairly constant compositions (Fig. 2), with only two samples showing wedges superimposed on a concentric growth zonation (Fig. 4). Concentric zonation is parallel to wedge bases but has an 'onlap' relationship with the top surfaces of wedges (Fig. 5). Individual wedges have a geometry as shown in Fig. 6. In 2D section paired wedges frequently propagate along a curved path (Fig. 3) and usually the top surface of one wedge is parallel to the bottom of the next (Fig. 3). Even where these surfaces are subparallel (usually when wedges show a relatively high degree of curvature; Fig. 7), there is an overall expansion of the crystal between the thin and thick ends of wedges. Wedges are generally only developed where there was a propagating edge; where an edge met an adjacent crystal, subsequent growth was wedge-free (Fig. 8). In extremely rare instances single wedge series occur adjacent to major crystal cleavage planes, rather than along propagating edges (Fig. 7). Wedges cannot be correlated between different parts of a single crystal or between adjacent crystals (Fig. 8).

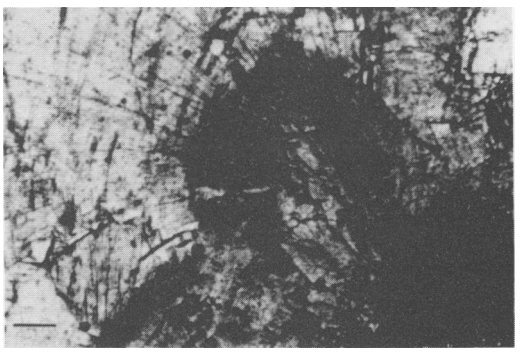

FIG. 1. Saddle dolomite in plane-polarized light (AS1); scale bar 0.5 mm.

At high magnifications BSEM images show that both wedges and, to a lesser extent, the host crystals have a streaky fabric. This fabric in the wedges comprises irregular, 0.1–2 μm diameter, flames of host crystal composition which are usually subparallel to the opposing face at the corner (Fig. 9). Streakiness within the host crystal parallels that within wedges and comprises laminae, less than 1 μm diameter, of slightly differing compositions. These streaky fabrics are the major cause of the analytical spread of the wedge and non-wedge compositions of individual samples (Fig. 2).

Wedges are always Mg enriched with respect to the bulk crystal (Fig. 2). Most samples show

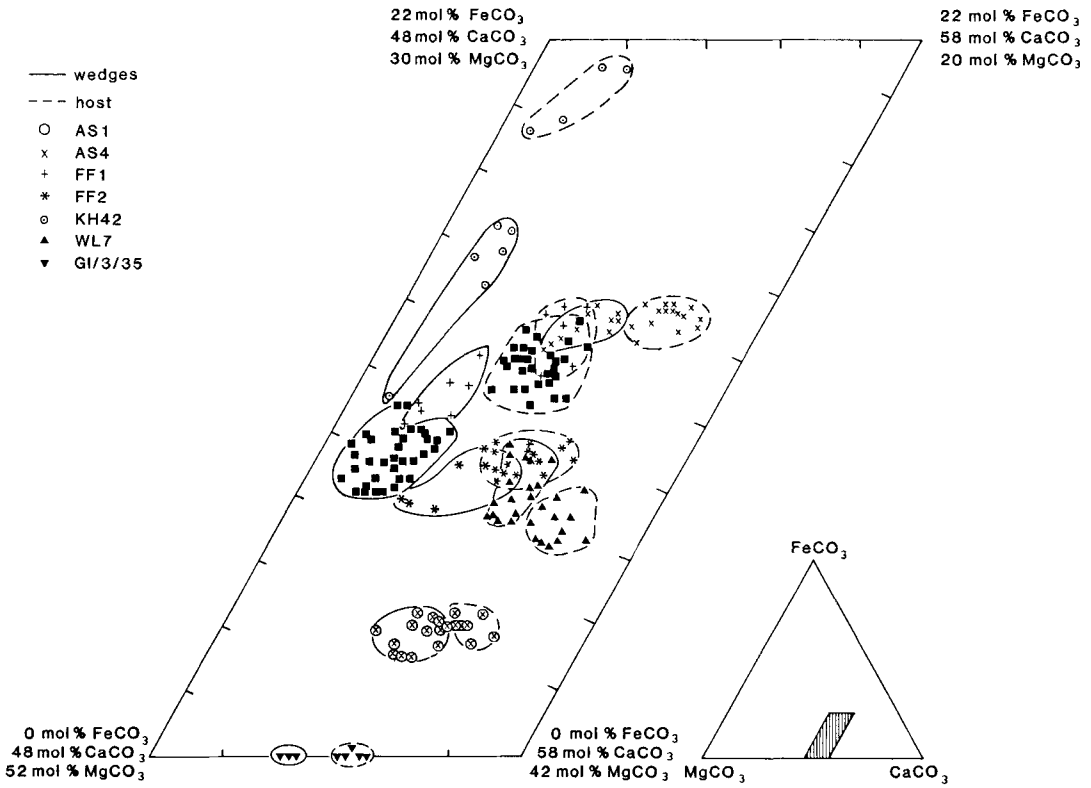

FIG. 2. Probe analyses of saddle dolomites: in all samples 'wedges' are Mg-enriched but Ca and/or Fe-depleted relative to the host crystal.

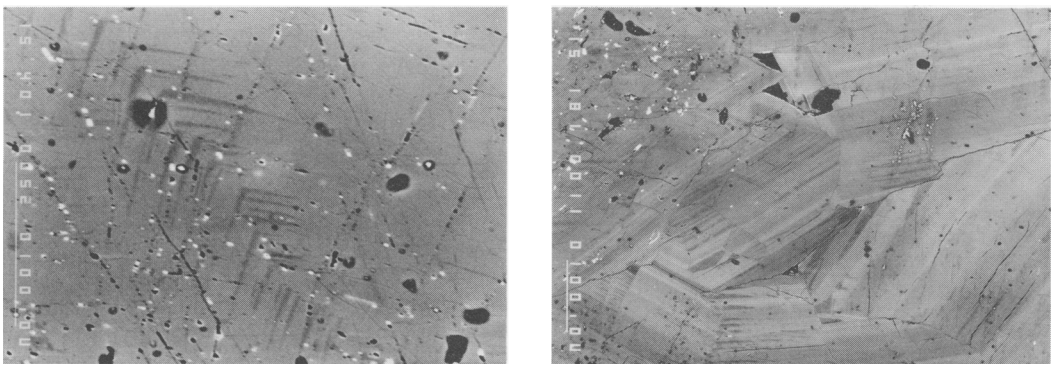

FIG. 3 (*left*). BSEM image of saddle dolomite (AS1) showing a series of paired Ca-depleted wedges (i.e. dark relative to host crystal) which have propagated along a curved path. FIG. 4 (*right*). Ca-depleted wedges superimposed on concentric compositional banding in saddle dolomite (BSEM, WL7).

a depletion in Fe and Ca in the wedges, a few with depletion only in Ca, and in a single instance depletion only in Fe. Mn contents of the crystals vary in a similar manner to Fe.

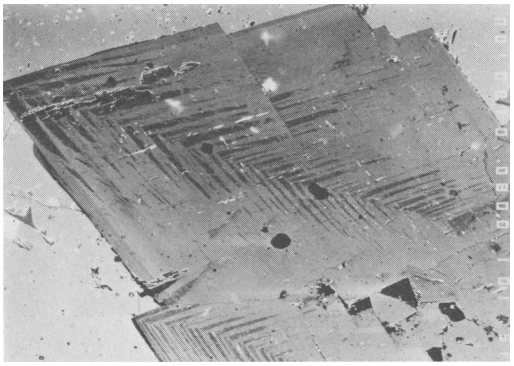

FIG. 5. Concentric growth zones 'onlapping' Ca-depleted wedges in the outer parts of a saddle dolomite crystal (BSEM, AS4).

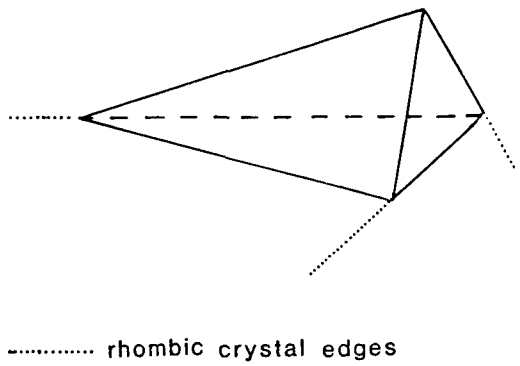

FIG. 6. Wedge geometry relative to rhombic dolomite faces.

Discussion

Finescale structure of saddle dolomites. The streaky BSEM fabric of saddle dolomites has a similar crystallographic orientation to the calcite laths observed in TEM by Barber *et al.* (1985), which suggests the two features are related. The presence of discrete calcite laths within the dolomite lattice cannot be the sole cause of distortion in saddle dolomite as carbonatite dolomite, without curved faces, shows similar TEM microstructures (Barber and Wenk, 1984). In addition, subsequent TEM work by Barber and Riaz Khan (1987) shows that similar two-phase microstructures are common in natural and synthetic carbonate minerals with a dolomite structure. The origin of such microstructures is not clear; although there are some morphological similarities to exsolution laminae, ionic diffusion rates in the dolomite lattice are too low at temperatures less than 200 °C for exsolution to occur (Barber *et al.*, 1985). Barber and Riaz Khan (1987) hint that the two-phase microstructures are primary features due to the small degree of calcite–dolomite solid solution at low temperatures. Calcic dolomites may, therefore, represent coprecipitated fine-scale intergrowths, rather than true solid solutions.

Barber *et al.* (1985) note that calcitic laths in saddle dolomite are unevenly distributed within the crystal, forming domains of varying lath density. The BSEM streakiness may be the manifestation of this variation, being due to variations in lattice strain in areas of differing lath density. In addition, there is the possibility that both wedge and host crystal compositions represent preferential levels of lath inclusion.

Solution control on dolomite composition. The accommodation of Ca and to a lesser extent Fe as a separate phase in dolomite on the nm scale probably has a relatively minor effect on bulk crystal composition, which is instead largely controlled by physical and chemical conditions prevailing in the precipitating solution. Controls include: fluid Mg/Fe/Ca ratios, (Mattes and Mountjoy, 1980), Eh, pH, the degree of supersaturation (Weaver, 1973) which controls crystal growth rate, and the differential complexing of Mg, Fe and Ca by other species in solution. At rapid growth rates dolomite will show an enrichment of Ca and slight enrichment of Fe over Mg as a consequence of the relative ease of dehydration of the three species: $Ca \gg Fe > Mg$. The degree of Ca and Fe enrichment is probably limited by the requirement to nucleate a second phase to accommodate them within the dolomite lattice. Temperature may also be important due to its effect on the differential activation energies of absorption and dehydration of Ca, Mg and Fe.

Origin of the wedges. Wedge geometry suggests that they are related to the development of curved crystal faces. Relative enrichment of the smaller Mg^{2+} over Ca^{2+} within the wedges makes it unlikely that the implied lattice extension is due to increased *d*-spacing. Instead the lattice extension must represent the incorporation of extra lattice layers within the wedges relative to face centres. To accommodate such extra layers, a high density of crystallographic dislocations must be present between wedge and non-wedge parts of the crystal. Published TEM data are compatible with, but, insufficient to confirm the presence of wedge-associated zones of high crystallographic dislocation density (Barber *et al.*, 1985).

The lack of correlation between wedges on

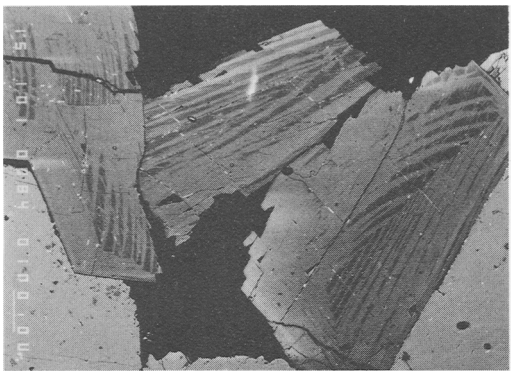

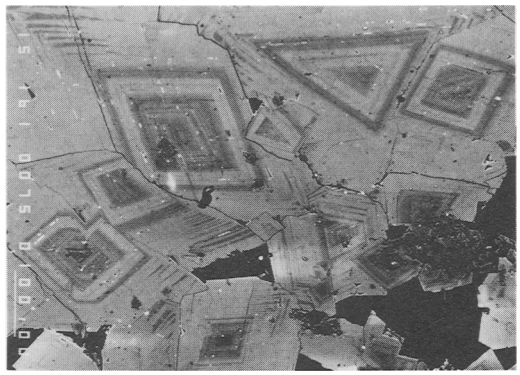

FIG. 7 (*left*). Wedges, both edge- and cleavage-associated types, with a high degree of curvature (BSEM, AS4).
FIG. 8 (*right*). Crystals showing wedge development during latest stages of growth; wedges do not correlate between crystals and are only developed at free edges and cleavage planes (BSEM, AS5).

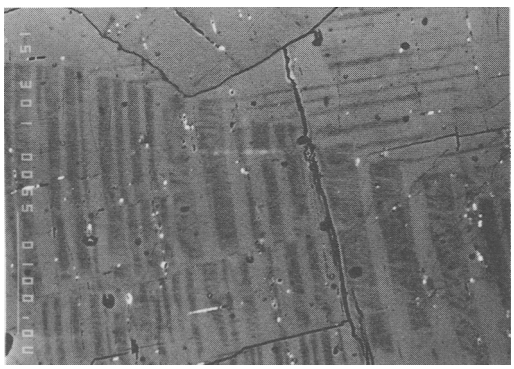

FIG. 9. Fine structure of wedges in which flames of host crystal composition are parallel to wedge development on the opposing crystal face (BSEM, AS5).

adjacent crystals indicates that they developed through a process acting immediately adjacent to growing crystal faces independent of conditions in the bulk pore. The frequent lack of overall compositional gradients within crystals suggests that bulk solution conditions were relatively stable. Both these factors indicate that solution chemistry immediately around growing crystals varied independently of bulk solution chemistry, and, therefore some kind of compositional boundary layer existed around growing crystals. The development of such a solution boundary layer requires that crystal growth rate is determined either by ionic supply or the removal of growth-inhibiting species. Mechanisms of supply and removal involve both pore-fluid through flow and ionic/molecular diffusion. In most diagenetic environments, other than within some active hydrothermal systems, fluid flow is considerably slower than rates of ionic diffusion (Giles, 1987). Even within hydrothermal systems, fluid flow immediately adjacent to cavity walls would be significantly reduced by friction. The absence of pronounced asymmetry of growth zones in the saddle dolomite suggests bulk fluid flow is unlikely to have been an important factor in wedge development.

The extra edge-associated lattice layers suggest that during wedge development lattice layers nucleated at crystal edges but failed to propagate across the entirety of the growing face before initiation of the next layer. In most aqueous systems, and certainly during rapid growth, crystals grow with continuous addition of material across the entirety of the growing 'surface-roughened' faces (Sunagawa, 1981, 1977). If supersaturation drops below a certain critical level, continuous growth is replaced by edge-nucleated growth (Sunagawa, 1977). The Mg-enrichment of wedges with respect to host crystals suggests slower growth rates than for host crystal growth (above), which is compatible with development by edge-nucleated growth within a depleted boundary layer. The rare instances of cleavage-associated wedges may be a function of the high density of crystallographic dislocations enhancing lattice layer nucleation along the propagating cleavage. The decrease in wedge width in the direction of edge propagation within individual wedges suggests that the rate of lattice propagation across the face decreased relative to layer nucleation rate as individual wedges developed. This suggests that supersaturation within the depleted boundary layer was progressively reduced during wedge development, such that the effects of more rapid ionic diffusion to the crystal edge over the face concentrated precipitation towards the edge. Alterna-

tively, instead of a supply-controlled growth model, the gradual build up of growth-inhibiting species would have a similar effect. The removal of the inhibiting species would be most rapid from crystal edges, which could allow continued nucleation of lattice layers at the edges after growth at face centres had been halted. Saddle dolomite growth, therefore, involves an oscillation between rapid continuous growth right across the crystal face and slower edge-nucleated growth. During continuous growth, wedges are engulfed by the advancing bulk crystal which gives rise to the onlap geometry of concentric growth zones against wedges. The difference in size between Ca^{2+} and Mg^{2+} and the accommodation of excess Ca within a discrete second phase, prevents complete matching of wedge and non-wedge parts of the crystal, and allows preservation of the extra lattice layers at face edges relative to face centres.

Oscillatory processes during crystal growth. Oscillatory compositional zonation occurs in several minerals; notably, oscillatory-zoned plagioclase is common in many igneous rocks. Plagioclase zonation does not involve the changing growth mechanism seen in saddle dolomites, but it does provide an analogous example of oscillatory growth thought to result from transport-controlled kinetics. At least three models have been proposed to explain the development of oscillatory zonation in plagioclase:

(1) Control of each lattice layer on the successive lattice layer's composition so that for most of the time surface composition is not in equilibrium with immediately adjacent solution (Haase *et al.*, 1980).
(2) The existence of a delay time between the change in supersaturation at the crystal face and a corresponding adjustment of growth rate (Allegre *et al.*, 1981).
(3) Compositionally-induced convection (Loomis, 1982; Martin *et al.*, 1987).

The first model may have some relevance to saddle dolomites, as excess Ca and Fe are accommodated in discrete second-phase defects (Barber *et al.*, 1985), and it is possible that such features have activation energies of opening and closure. If such activation energy barriers exist, the cationic chemistry of individual lattice layers would be partly controlled by the pre-existing intergrowth structure. However, this lattice-controlled model should produce a succession of several crystal compositions, as opposed to the observed abruptly biomodal pattern of compositional variation. More significantly, it does not explain the oscillation between continuous and edge-nucleated growth. The second model is also difficult

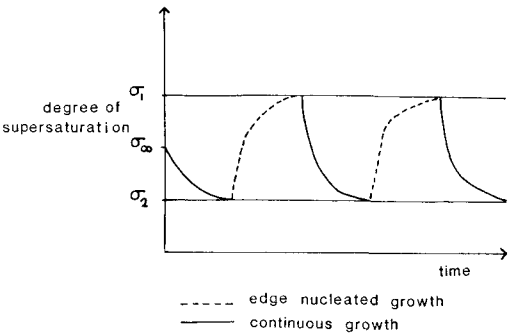

FIG. 10. Model of the evolution of boundary layer chemistry through time to generate continuous oscillation between edge-nucleated and surface-roughened continuous growth mechanisms. It is assumed that growth is transport-controlled and that there is a delay between changing levels of supersaturation at the growing crystal face and a corresponding change in growth mechanism. σ_∞ = saturation level of the bulk solution, precisely at edge-nucleated/continuous growth boundary, σ_1 = saturation above which all growth is continuous, σ_2 = boundary above which all growth is edge-nucleated. Initially the boundary layer is sufficiently supersaturated for rapid continuous growth, with crystal growth outpacing ionic supply. Supersaturation of the boundary layer drops to a critical level, σ_2, at which continuous growth can no longer occur, and further lattice layers can only be added by edge nucleation. During edge-nucleated growth supply is more rapid than crystal growth and supersaturation of the boundary layer builds up until it reaches σ_1. At this point the crystal face then reverts to continuous rapid growth and the process is reinstigated.

to apply directly to saddle dolomite because precipitation rate will continually adjust to supersaturation at the crystal surface; this suggests, as in the first model, that continuous rather than abruptly bimodal discontinuous compositional variation should result. Additionally, in order to maintain an oscillation between edge-nucleated and continuous growth, the bulk solution would need to have a level of supersaturation precisely at the edge-nucleation/continuous growth boundary. Such conditions are likely to be very restricted, which contrasts with the abundance of saddle dolomite in the geological record. A development of the second model, combined with the first model, in which there is a sharp break in growth rate between edge-nucleated and continuous growth, combined with a delay in switching from one growth mechanism to the other, might generate oscillatory growth (Fig. 10). As in the more direct application of the second model, the stable oscillation of growth modes would require

quite exacting solution conditions and there would appear to be a high probability than oscillation would decay during progressive crystal growth. This contrasts with observed patterns of wedges (Figs 3, 8). The implied slight increase in growth rate as supersaturation builds up during edge-nucleated, wedge-developing growth is also inconsistent with wedge geometry (above). The third model, invoking compositional convection, would appear the most likely main cause of oscillatory growth in saddle dolomite because of the relative simplicity of conditions required to generate a buoyant compositional boundary layer around crystals. Supersaturation merely has to be sufficient such that crystal growth rate outpaces ionic diffusion.

Compositional convection. Within crystallizing magmas the depleted boundary layer generated by crystallization is large relative to crystal size, whereas in aqueous systems the depleted boundary layer generated by crystallization is small relative to crystal size (Martin *et al.*, 1987). This suggests that, in the case of saddle dolomites, boundary layer effects will be controlled entirely by individual crystals rather than operating on the pore-size scale, consistent with the non-correlation of wedges between crystals of saddle dolomite. Martin *et al.* (1987) suggest that during crystal growth from aqueous solution, the depleted solution clings to the growing crystal faces and is drawn up to form a stable convective plume above the highest corner. This leads to elongate crystal morphologies which contrasts with the generally equant morphologies of saddle dolomite. However, several features would appear to destabilize a convection plume as envisaged by Martin *et al.* (1987). Firstly, diffusion of ions to crystal vertices is much more rapid than to the centre of faces and this must lead to complex interactions of diffusion versus convective flow above the highest corner. Secondly the boundary layer has to attain a critical thickness for convection to occur. Not only must the critical compositional Rayleigh number be exceeded, but there are presumably surface tension effects between depleted and bulk fluids to be overcome. Once this critical volume has been exceeded, a relatively large bubble of depleted boundary layer fluid might detach itself from the highest point of the crystal to leave a boundary layer too thin for the continuation of convective flow. An analogous process can be observed when sugar cubes are dissolved immediately above a drop: the sinking plume of sugar solution is released in pulses from the sugar cube's boundary layer. A third factor which might prevent establishment of a stable convection plume is the possible interaction of convection-driven flow adjacent to crystals with fluid flow in the main body of the cavity. Fourthly, crystal growth will not only generate compositional bouyancy effects, but also minor thermal bouyancy. Convection driven by coupled compositional and thermal bouyancy effects, where compositional bouyancy is the predominant force, is generally unstable (Turner, 1979). Overall it would seem that unstable compositional convection is potentially a mechanism by which oscillatory behaviour might be generated during precipitation of saddle dolomite.

An initial assessment of the probable importance of compositional convection during precipitation of saddle dolomite can be made by estimating the thickness of the compositional boundary layer above a horizontal crystal surface required for convective overturn to occur during the precipitation of dolomite from sea-water (see Appendix). Sea-water is considerably more dilute than the hydrothermal and deep diagenetic brines generally associated with saddle dolomite, so that in reality the critical thickness of the boundary layer at which convection would occur above a flat face should be somewhat less than the 3.3 mm required in seawater. More importantly, consideration of convection above a horizontal face is geologically unrealistic. If a buoyant boundary layer developed above inclined crystal faces is drawn up towards the highest crystal corner (Martin *et al.*, 1987), then presumably the critical thickness relevant to the occurrence or absence of compositional overturn would be of the same order of magnitude as crystal size. The implication that crystals have to attain a critical size before wedge development occurs is consistent with the relatively coarsely crystalline nature of saddle dolomite (Radke and Mathis, 1980) and the absence of wedge development during the early growth stages of crystals illustrated in Fig. 8.

Model for wedge formation in saddle dolomite. Saddle dolomite growth is controlled by rates of solute supply which allow a compositionally bouyant solution boundary layer to develop adjacent to the growing crystal. This bouyant surface layer of solution is held to the growing crystal by surface tension, and thickens during progressive crystal growth. Ultimately a critical point is reached at which bouyancy is sufficient to overcome surface tension effects and a bubble of depleted fluid escapes from the growing crystal allowing fresh solution to reach the crystal face. Continuous growth operates during the early post-replenishment part of each cycle and is replaced by edge nucleation once the boundary layer has evolved to a critical level of solute depletion. Supersaturation, and therefore growth rates, fall

continuously subsequent to the initiation of each cycle.

The control of growth rate on dolomite Mg/Ca/Fe ratios might be expected to produce continuous compositional gradients within saddle dolomites during each growth cycle. The absence of such continuous zonation may be due to a very sharp change in growth rates when growth mechanism changes, with falling growth rate otherwise having a very small effect. Alternatively, or additionally, there might be temperature-dependent compositional gaps in Mg–Ca–Fe solid solution, related to the accommodation of the sub-micron scale calcite laths (Barber *et al.*, 1985) into the dolomite structure. The composition of each lattice layer is possibly strongly influenced by the preceding layer (see above) and it may require the change in growth mechanism to trigger the jump to a different lattice layer composition.

Diagenetic significance of saddle dolomite

The proposed ionic supply control on saddle dolomite growth kinetics contrasts strongly with crystal growth in other diagenetic environments in which growth rates are controlled by surface kinetics (Berner, 1983). Saddle dolomite must, therefore, precipitate under conditions of extreme supersaturation or in environments where surface-related activation energy barriers are much reduced. The actual rates of dolomite growth indicated are difficult to calculate because the ideal conditions for dolomite growth are unknown (Hardie, 1987). However, for the hypothetical precipitation of dolomite from seawater at 25 °C, an ionic-supply controlled growth rate can be estimated. In seawater, as in most diagenetic fluids, CO_3^{2-} is depleted relative to Ca^{2+} and Mg^{2+}, and, therefore, is the rate-determining species. If all available CO_3^{2-} (0.3 mM) was utilized, the dolomite growth rate would be slightly greater than 5.9 mm^2 $year^{-1}$ (Appendix). Actual natural dolomite growth rates are difficult to assess: modern near-surface dolomite is extremely fine-grained and often occurs as metastable protodolomite (e.g. Butler *et al.*, 1982). In addition, it has not been possible to synthesize ordered, stable dolomites in the laboratory at temperatures less than 200 °C (Hardie, 1987). Deep subsurface dolomites, thought to have precipitated in less than 20 years, form rhombs only 20 μm diameter (Boles, 1987). The proposed rate of transport-controlled precipitation of dolomite from sea-water is however slower than rates of modern $CaCO_3$ tufa accumulation around hot springs (Folk *et al.*, 1985).

Conclusions

Lattice distortion in saddle dolomites is caused by the incorporation of extra lattice layers at propagating crystal edges, relative to face centres. These extra layers are visible in BSEM as Mg-enriched wedges developed along propagating edges. The non-correlation of the wedge-shaped extra zones between adjacent crystals implies that crystal growth kinetics were controlled by rates of ionic transport. It is suggested that the wedges reflect switching from continuous growth across crystal faces to edge-nucleated growth. Oscillatory behaviour is possibly generated through compositional convection. Saddle dolomite growth rates appear, therefore, to be extremely rapid compared with normal diagenetic mineral growth, but a full understanding of the growth conditions will require some complex mathematical modelling.

Acknowledgements

I thank the Geology Department of St Andrews University for extensive use of their microprobe, with particular thanks to Donald Herd and Ed Stephens for their help. I also thank Colin Donaldson for his help and encouragement during the course of this study.

References

Atkins, P. W. (1986) *Physical Chemistry* (3rd Edn).

Allegre, C. J., Provost, A. and Jaupart, C. (1981) *Nature* **294,** 223–8.

Barber, D. J. and Riaz Khan, M. (1987) *Mineral. Mag.* **51,** 71–86.

——and Wenk, H. R. (1984) *Contrib. Mineral. Petrol.* **88,** 233–45.

——Reeder, R. J. and Smith, D. J. (1985) Ibid. **91,** 82–92.

Berner, R. A. (1983) In *Kinetics of Geochemical Processes* (A. C. Lasaga and R. J. Kirkpatrick, eds.). *Reviews in Mineralogy*, Min. Soc. Am., **8,** 111–34.

Boles, J. R. (1987) In *Diagenesis of sedimentary sequences* (Marshal, J. D., ed.). Spec. Publ. Geol. Lond. **36,** 191–200.

Butler, G. P., Harris, P. M. and Kendal, G. C. St. C. (1982) In *Deposition and diagenetic spectra of evaporites* (C. R. Handford, R. G. Loucks and G. R. Davies, eds.). Soc. Econ. Paleont. Mineral. Core Workshop **3,** 33–64.

Deer, W. A., Howie, R. A. and Zussman, J. (1966) *An introduction to the rock-forming minerals.* Longman.

Folk, R. L., Chafetz, H. S. and Tiezzi, P. A. (1985) In *Carbonate Cements* (N. Schneidermann and P. M. Harris, eds.). Soc. Econ. Mineral. Paleont. Spec. Publ. **36,** 349–70.

Giles, M. R. (1987) *Marine Petrol. Geol.* **4,** 183–204.

Haase, C. S., Chadam, J., Feinn D. and Ortoleva, P. (1980) *Science* **209,** 272–4.

Hardie, L. A. (1987) *J. Sed. Petrol.* **57,** 166–83.
Hird, K., Tucker, M. E. and Waters, R. A. (1987) In *European Dinantian Environments* (J. Miller, A. E. Adams and V. P. Wright, eds.), 359–78.
Krauskopf, K. B. (1979) *Introduction to Geochemistry* (2nd Edn).
Loomis, T. P. (1982) *Contrib. Mineral. Petrol.* **81,** 219–29.
Martin, D., Griffiths, R. W. and Campbell, I. H. (1987) Ibid. **96,** 465–75.
Mattes, B. W. and Mountjoy, E. W. (1980) In *Concepts and Models of Dolomitization* (D. H. Zenger, J. B. Dunham and R. L. Ethington, eds.). Soc. Econ. Mineral. Paleont. Spec. Publ. **28,** 123–37.
Radke, B. M. and Mathis, R. L. (1980) *J. Sed. Petrol.* **50,** 1149–68.
Sunagawa, I. (1977) *J. Crystal Growth* **42,** 214–23.
——(1981) *Bull. Mineral.* **104,** 81–7.
Turner, J. S. (1979) *Bouyancy effects in fluids.* Cambridge Univ. Press, 368pp.
Weaver, C. E. (1973) *Geology*, **3,** 425–9.

[*Manuscript received 23 January 1989; revised 11 April 1989*]

Appendix

Calculation of boundary layer thickness required for compositional overturn to occur during precipitation of dolomite from seawater. Compositional convection occurs within a system if its Ra_s, compositional Rayleigh number, is greater than 1000. Ra_s is dependent on the vertical thickness of the system. It is, therefore, possible to calculate the minimum boundary layer thickness above a flat crystal face, for given compositions of bulk solution and at the crystal face, within which convective overturn could occur.

$$Ra_s = \frac{g\beta\Delta S h}{\nu K_s} = \frac{g(p-p_o)h}{K_s}$$

where g = acceleration due to gravity, β = compositional thermal expansion coefficient, ΔS = concentration change, h = vertical thickness of boundary layer, ν = kinematic viscosity and K_s = concentration diffusion coefficient. $p-p_o$ = change in seawater density due to dolomite precipitation.

In seawater CO_3^{2-} is depleted relative to Ca^{2+} and Mg^{2+} so that CO_3^{2-} diffusion would be rate limiting during dolomite precipitation. Therefore K_s is taken to be the diffusion coefficient of CO_3^{2-} at 25 °C = 9.58×10^{-6} $cm^2\ s^{-1}$ (calculated from data tabulated in Atkins, 1986) η is taken as 1.02×10^{-2} g $cm^{-1}\ s^{-1}$ (data for NaCl solution, International Critical Tables) $p-p_o$ is approximated as the density of seawater – (density of seawater – 0.15 mM dolomite $\times 10^{-3}$) = 27.6×10^{-6} g cm^{-3} where 0.15 mM dolomite represents concentration of dolomite in seawater, utilizing all available CO_3^{2-}

If $Ra_s > 1000$

$$h > \sqrt[3]{\frac{\eta K_s}{g(p-p_o)}}$$

$$= \sqrt[3]{\frac{1000 \times 1.02 \times 10^{-2} \times 9.58 \times 10^{-6}}{100 \times 27.6 \times 10^{6}}}$$

$$= 0.328 \text{ cm}$$

$h > 3.28$ mm

Hence during diffusion-controlled growth of dolomite from seawater, convective overturn of a depleted boundary layer could occur once that layer had evolved to a thickness greater than 3.3 mm.

Dolomite growth rate from seawater. If CO_3^{2-} (aq) supply is rate determining, the concentrations of Mg^{2+}, Ca^{2+} and Fe^{2+} in solution at the crystal face must be equivalent to those in the bulk solution. In seawater the ionic activity product (IAP) of dolomite is 10^{-15}, the solubility constant (K) is 10^{-17} and the concentration of CO_3^{2-} is 0.3 mM (data tabulated by Krauskopf, 1979). Assuming that the solution at the growing face is at equilibrium concentration: $[CO_3^{2-}]_{FACE} = [CO_3^{2-}]_{SOL} \times K/IAP$

$$= 0.3 \times 10^{-5} \text{ M}$$

The diffusion coefficient of CO_3^{2-} at 25 °C = 0.58×10^{-6} $cm^2\ s^{-1}$ (calculated from data tabulated in Atkins, 1986). Molar density of dolomite = 1.55×10^{-2} mol cm^{-3} (calculated from data tabulated in Deer *et al.*, 1966).

For crystal growth governed by CO_3^{2-} diffusion:

$$\text{growth rate} = \frac{D([CO_3^{2-}]_{SOL} - [CO_3^{2-}]_{FACE})}{\text{molar density dolomite}}$$

$$= 1.85 \times 10^{-9} \text{ cm}^2\text{ s}^{-1}$$

$$= 5.85 \times 10^{-2} \text{ cm}^2 \text{ year}^{-1}$$

This estimate is slightly too small because it does not allow for the effect of the dolomite growth front advancing into the solution.